Kuyper, B., Lesch, T., Labuschagne, C., Martin, D., Young, D., Khan, M. A. H., Williams, A. G., O'Doherty, S., Davies-Coleman, M. T., & Shallcross, D. E. (2019). Volatile halocarbon measurements in the marine boundary layer at Cape Point, South Africa. *Atmospheric Environment*, *214*, [116833]. https://doi.org/10.1016/j.atmosenv.2019.116833

Volatile halocarbon measurements in the marine boundary layer at Cape Point, South Africa

Brett Kuyper[a], Timothy Lesch[a], Casper Labuschagne[b], Damien Martin[c], Dickon Young[c], M. Anwar H. Khan[c], Alastair G. Williams[d], Simon O'Doherty[c], Michael T. Davies-Coleman[a] and Dudley E. Shallcross[a,c,*]

[a] Department of Chemistry, University of the Western Cape, Robert Sobukwe Rd, Bellville 7535, South Africa
[b] Climate and Environmental Research and Monitoring, South African Weather Service, Stellenbosch 7600, South Africa
[c] Atmospheric Chemistry Research Group, School of Chemistry, University of Bristol, Cantock's Close, Bristol, BS8 1TS, United Kingdom
[d] Australian Nuclear Science and Technology Organisation, Locked Bag, 2002 Kirrawee DC, NSW, 2232, Australia
[*]Corresponding author: email: d.e.shallcross@bristol.ac.uk, Tel: +44 117 928 7796

Abstract

Volatile organic halocarbons play a significant role in the biogeochemical cycling of halogens in the atmosphere. High frequency, *in situ* measurements of methyl iodide (CH_3I), bromoform ($CHBr_3$), dibromomethane (CH_2Br_2) and methyl bromide (CH_3Br) were measured in the marine boundary layer at Cape Point, South Africa by an automated Absorption Desorption System-Gas Chromatography-Mass Spectrometer (ADS-GC-MS) between January and November 2017. These are the first multi-halocarbon measurements recorded at Cape Point and represent the longest time series to date. Baseline wind conditions were established using both wind direction and radon (^{222}Rn) concentration as markers of clean air. The baseline mixing ratios observed were 0.61 ± 0.29, 2.02 ± 0.89, 1.08 ± 0.17 and 6.09 ± 0.50 ppt, for CH_3I, $CHBr_3$, CH_2Br_2, and CH_3Br, respectively. A statistically significant difference in short-lived halocarbon occurrence was established between anthropogenically affected and clean marine air masses for CH_3Br at the Cape Point site. The $CHBr_3$ and CH_2Br_2 mixing ratios were not statistically different ($p > 0.05$) when comparing the anthropogenically affected and clean marine air masses. The mixing ratios of CH_3I suggested a strong seasonal variation with higher production in austral Summer-Autumn months than in the austral Winter-Spring months. A general chemical decay line was calculated for baseline CH_2Br_2 and $CHBr_3$ measurements at Cape Point. An analysis of the $\ln([CH_2Br_2]/[CHBr_3]):\ln([CHBr_3])$ ratio for the Cape Point dataset exhibited a slight

deflection to the right of the general chemical decay line, suggesting the influence of greater [$CHBr_3$]:[CH_2Br_2] source ratios rather than their dilution.

Keywords:
Bromoform; methyl bromide; dibromomethane; methyl iodide; marine air

1. Introduction

Volatile organic halocarbons e.g. CH_3I, $CHBr_3$, CH_2Br_2 and CH_3Br, are pivotal to the biogeochemical cycling of halogen species between the ocean and the atmosphere (Quack and Suess, 1999; Quack and Wallace, 2003; Carpenter and Nightingale, 2015). Some of these halocarbons, e.g. CH_3I, $CHBr_3$ and CH_2Br_2 form part of a suite of atmospheric trace gases known as very short-lived substances (VSLS), with comparatively short atmospheric lifetimes of days to months (Carpenter and Liss, 2000; Montzka and Reimann, 2011; Carpenter and Reimann, 2014; Carpenter and Nightingale, 2015). VSLS which are mainly produced in the ocean, are outgassed into the marine boundary layer. The lifetimes of CH_3I (~ 4 days), $CHBr_3$ (~15 days), CH_2Br_2 (~94 days) and CH_3Br (~292 days) are long enough to allow them to be transported to the free troposphere and in some cases subsequently the stratosphere via deep convection events (Montzka and Reimann, 2011; Carpenter and Reimann, 2014; Fuhlbrügge et al., 2016). Transport into the free troposphere is significantly enhanced over the tropical oceans through tropical storms and cyclones (Krüger and Quack, 2013; Carpenter and Reimann, 2014; Fuhlbrügge et al., 2016). Reactive bromine and iodine radicals, released from the photolytic degradation of photolabile VSLS, may contribute to catalytic destruction cycles leading to ozone depletion in both the stratosphere and troposphere (Vogt et al., 1999; Carpenter and Liss, 2000; Montzka and Reimann, 2011; Saiz-Lopez et al., 2012; Carpenter and Reimann, 2014). In the marine boundary layer, catalytic ozone depletion can be initiated by reaction with IO, which can also modify the OH/HO_2 and NO/NO_2 cycles (Read et al., 2008; Jones et al., 2009). The atmospheric lifetimes of several climatically important trace gases (e.g. CH_4, CO_2) are controlled by the OH/HO_2 and NO/NO_2 cycles (Vogt et al., 1999; Carpenter, 2003; Bloss et al., 2005; Read et al., 2008; Jones et al., 2009).

Until recently, it was postulated that stratospheric loading of inorganic bromine with mixing ratios of 22.5 ppt (range of 19.5 to 24.5 ppt) was thought to be derived mostly from long-lived (>

6 months) bromocarbon species e.g. CH_3Br, H-1211 and H-1301 (Montzka and Reimann, 2011; Aschmann and Sinnhuber, 2013; Robinson et al., 2014). However, attention is increasingly being focused on short-lived biogenic VSLS as evidence mounts from both observations and modelling studies that other, as yet undetermined, biogenic sources of VSLS must contribute to atmospheric bromine mixing ratios (Fuhlbrügge et al., 2016; Yokouchi et al., 2017). The biogenic sources contribute ~50% of the bromine present in the atmosphere and the global contribution to stratospheric halogen loading from the VSLS bromine compounds is estimated at 5 ppt (range of 2 to 8 ppt) (Carpenter and Reimann, 2014).

The main sources of biogenic VSLS and CH_3Br, reported are marine macroalgae and phytoplankton, with the former a more prolific source than the latter (Manley et al., 1992; Carpenter and Liss, 2000; Jones et al., 2009). Based on laboratory studies and *in situ* assessments (Manley and Dastoor, 1987; Ginger et al., 1992; Manley et al., 1992; Goodwin, 1996), Goodwin et al. (1997) estimated the emissions of $CHBr_3$, CH_2Br_2 and CH_3Br into the atmosphere from macroalgae e.g. kelp, as 3.1– 48 Gg Br yr^{-1}. Non-kelp macroalgae are projected to contribute a further 0.82 – 32 Gg Br yr^{-1} into the atmosphere, via $CHBr_3$ and CH_2Br_2, with an additional 9.5 – 140 Gg Br yr^{-1} discharged as $CHBr_3$ from polar macroalgal communities (Goodwin et al., 1997). Coastal populations of marine phytoplankton are reported (Sæmundsdóttir and Matrai, 1998) to be one of the major sources of CH_3Br (1.21 – 3.72 Gg Br yr^{-1}, Manley and Dastoor, 1987; Reeves and Penkett, 1993; Butler, 1995).

The ocean is the main source of the volatile iodinated compounds present in the atmosphere. The production of CH_3I by macroalgae and ice algae from coastal and polar regions respectively, is well established (Carpenter et al., 1999; 2000; Giese et al., 1999). Open ocean phytoplankton species e.g. *Prochlorococcus sp.* have also been shown to be contributors to the estimated global flux of 0.6 Mmol CH_3I yr^{-1} (Brownell et al., 2010). The photochemical production of CH_3I in the open ocean has been widely hypothosised (e.g. Happell et al., 1996; Palmer and Reason, 2009; Stemmler et al., 2014). The photolytic production of CH_3I is assumed to be proportional to the solar radiation and the amount of dissolved marine organic matter (Moore and Zafiriou, 1994; Happell and Wallace, 1996). Therefore, photolytic production may be important in the open ocean, away from high planktonic concentrations associated with coastal and nutrient rich upwelling regions (Moore and Zafiriou, 1994; Happell and Wallace, 1996).

There are also significant additional terrestrial contributions, both natural and anthropogenic, to the global input of CH_3Br including *inter alia* wild fires and biomass burning (Manö and Andreae, 1994; WMO, 1995), tropical plants, fungus, and leaf litter (Lee-Taylor and Holland, 2000), motor vehicle emissions, as well as general industrial activities (Khalil et al., 1993). The discharge into the atmosphere from the agricultural practice of large scale soil fumigation has been phased out under the Copenhagen Amendment to the Montreal Protocol (Yvon-Lewis et al., 2009; Carpenter and Reimann, 2014). The mean tropospheric CH_3Br mixing ratios had dropped to 7.0 ± 0.1 ppt by 2012 due to the implementation of the Montreal Protocol. One major exception to the ban on CH_3Br use was in the form of quarantine and pre-shipment (QPS) fumigation with no substantial change in emissions for QPS purposes since then (Carpenter and Reimann, 2014). Thus QPS fumigation would appear to be the dominant anthropogenic source to the atmosphere. Furthermore, the oceanic source and sink for CH_3Br have become comparable in magnitude (Carpenter and Reimann, 2014). Coastal nuclear power stations are suggested to be an additional minor anthropogenic source of $CHBr_3$. In nuclear power stations, $CHBr_3$ is a by-product from the reaction of HOCl (produced during the chlorination process used to prevent fouling of seawater fed cooling condensers), with bromine and dissolved organic matter (humus) in the coolant seawater (Quack and Wallace, 2003; Yang, 2001).

Our understanding of the sources and sinks of these biogenic halocarbons and their contributions to regional and global atmospheric halogen budgets, remains limited (Ziska et al., 2013). Regional and global models are mostly used to address the deficiencies in physical data measurements of these compounds in the atmosphere (e.g. Palmer and Reason, 2009; Hossaini et al., 2010; 2013; 2015; Ashfold et al., 2014). However, these models *a-priori* sources emerging from the oceans surrounding South Africa are still largely unknown. High frequency *in-situ* measurements of anthropogenic and biogenic halocarbons at the Cape Point Global Atmospheric Watch (GAW) station are the first of its kind from southern Africa. There has been one recent short-term study of atmospheric $CHBr_3$ mixing ratios at Cape Point (Kuyper et al., 2018) but more extensive data of are required.

The GAW station is situated in a region of high marine biomass and biodiversity of largely endemic marine species arising from the unique arrangement of the large, warm Agulhas current flowing to the south and the cold Benguela, a northward-flowing current to the west. In addition, sporadic upwelling events of nutrient rich cold water occur as part of the Benguela system along

the west coast of the Cape Peninsula to Namibia. Due to the seasonal wind directions, these events happen more predictably in summer. Cold, nutrient rich water is drawn to the surface and these events contribute to the rich biodiversity of largely endemic marine species found in this region (Pitcher et al., 1992; Sakko, 1998; Louw et al., 2016). Extensive kelp beds, contribute significantly to the biomass and are found along the entire west coast of South Africa, including Cape Point (Anderson et al., 2007). Some of these kelp beds are exposed to the atmosphere during low tide. The production of VSLS by marine macroalgae have been shown to increase during periods of partial desiccation and oxidative stress (Nightingale et al., 1995; Jones et al., 2009; Bravo-Linares et al., 2010). Carpenter et al., (2009) have also drawn attention to the possible impact of different marine environments on VSLS production. Sea-air fluxes of VSLS from four different marine environments are proposed to decrease as follows: coastal > upwelling waters > continental shelf > open ocean (Carpenter et al., 2009). The production of VSLS from the rich algal biodiversity around the Cape peninsula is hitherto unknown and this study makes a first contribution to our understanding of possible new sources of these compounds.

2. Experimental

2.1 Cape Point Sampling site

The Cape Point Global Atmospheric Watch (GAW) station (34.5 ºS 18.2 ºE) is situated in a nature reserve approximately 60 km south of the city of Cape Town on a high point (230 m above sea level) adjacent to the south western tip of Africa. The latitude of the station also closes, in part, a southern hemisphere latitudinal gap in atmospheric trace gas measurement sites between Cape Matatula (14 ºS, 171 ºW) in American Samoa and Cape Grim (41 ºS, 145 ºE) in Tasmania, Australia (Brunke and Halliday, 1983). More details about the site description can be found in Labuschagne et al. (2018).

The site of the GAW station receives clean marine air from the south Atlantic and Southern Ocean *via* strong south easterly to south westerly winds, especially dominant in the austral summer (Brunke et al., 2004; Labuschagne et al., 2018, Fig. 1a) due to the presence of the South Atlantic High Pressure system situated south west of the sub-continent from November to May

(Preston-Whyte and Tyson, 1993; Garstang et al., 1996; Tyson and Preston-Whyte, 2000). The retreat of the South Atlantic High Pressure system towards the equator during the austral winter (June to August, Preston-Whyte and Tyson, 1993; Garstang et al., 1996) results in the intensification of westerly and north westerly winds (Fig. 1b); often bringing rain to the Cape peninsular (Brunke et al., 2016). North westerly winds also occasionally deliver polluted air from the city of Cape Town to the Cape Point GAW station (Brunke et al., 2016).

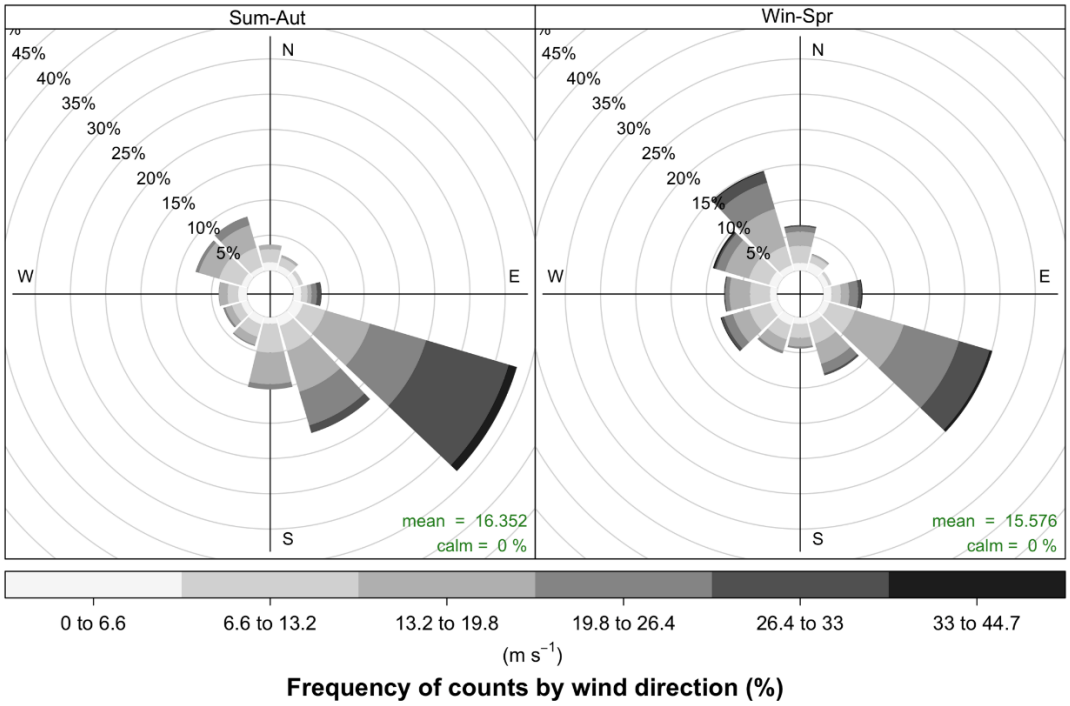

Fig. 1. Wind roses of the wind speed and direction over the two sampling periods at Cape Point in 2017. a) Sum-Aut (January – May); b) Win-Spr (June – November).

2.2. Measurement Technique

The Agilent 6890/5973 Gas Chromatograph-Mass Spectrometer (GC-MS) deployed to Cape Point for the analysis of air samples was fitted with a customised adsorption desorption system (ADS) and had been used extensively at Mace Head, Ireland (53 ºN, 10 ºW) (Simmonds et al., 1995). The ADS autonomously pre-concentrated and injected air samples and calibration standards onto a J&W Scientific CP Sil-5 (100 m x 0.32 x 5 µm) GC column. A micro trap, containing a triple adsorbent bed comprised of Carbotrap B (3 mg), Carboxen 1003 (5 mg) and Carboxen 1000 (4 mg) (O'Doherty et al., 1993; Sturrock et al., 2001), was cooled to -50 ºC using

triple cascade Peltier plates during the trapping phase (Sturrock et al., 2001). Direct ohmic heating was applied to the trap to raise the temperature to 240 °C and desorb compounds directly on to the head of the column. Initially the GC-MS was set to analyse samples under total ion chromatogram (TIC) to allow for the identification of compounds based on their full breakdown spectra and retention times. Using the target and qualifier ion information gained from the TIC analysis the GC-MS was set to single ion monitoring (SIM) mode for subsequent analyses (Table 1). SIM mode still allows discrimination between co-eluting species, by selectively focusing only on a few ions a better signal to noise ratio is obtained for the species of interest resulting in more precise measurements. A carrier gas flow rate (helium 5.0, Air Liquide) of 1.8 ml min^{-1} was used to elute the halocarbons controlled by a temperature programme with both isothermal (30 ºC, 12 min.) and temperature gradient (10 ºC min^{-1} to 150 ºC) periods.

Table 1. Target ion and qualifier ions for analysis and monitoring.

Compound	Target Ion	Qualifier Ion(s)	Precision (RSD)
CH_3I	127	-	5.14 %
$CHBr_3$	173	171	1.90 %
CH_2Br_2	174	93, 94	2.47 %
CH_3Br	94	96, 81	2.27 %

Samples were drawn from the atmosphere at ~17 l min^{-1} through a 15 m x ¼" OD stainless steel sampling line by means of a diaphragm pump (GAST, Miniature Diaphragm Pump 22D), with excess gas vented. Dust and rain were excluded from the sampling line *via* an inverted stainless steel cup system at the head of the sampling line at 4 m above ground level.

A standard tank (34 l, Essex Cryogenics), was filled at Mace Head, under baseline conditions, using a clean compressor (HSM Engineering, Authentic Air Compressor, model 1S3B-6EH-AQS, a version of the Rix Industries, USA, model SA-6 compressor built under license in the UK) in early 2017, following Fraser et al. (1999), Prinn et al. (2000), and Sturrock et al. (2001). The tank was analysed at Mace Head on an Advanced Global Atmospheric Gases Experiment (AGAGE) Medusa GC-MS (Miller et al., 2008; Arnold et al., 2012) to assign calibrated mixing ratios. This provides a direct comparison for CH_3Br against the AGAGE SIO-05 scale. $CHBr_3$, CH_2Br_2 and CH_3I are calibrated *via* AGAGE tank comparisons to National Oceanic and Atmospheric Administration (NOAA) calibration scales in Boulder ($CHBr_3$, NOAA-2003;

CH_2Br_2, NOAA-2003; CH_3I, NOAA-2004) using SIO tanks T-005B, T-009B and T-102B. Following calibration at Mace Head, the standard tank was shipped to South Africa in mid-2017 for use as a local long- term reference standard.

A short term working standard tank (34 l, Essex Cryogenics) was filled at Cape Point with a clean Rix compressor (SA-6AE), under baseline conditions (wind direction 120º-320º and ^{222}Rn < 350 mBq m^{-3}). During filling, the air was dried using Drierite (anhydrous calcium oxide) to ensure a water content of < 2 ppm in the working standard tank (Prinn et al., 2000). The cylinder was stored for three weeks prior to sampling, to allow for equilibrium of the trace gases. The short-term working standard was calibrated fortnightly over a 48 hour period against the long-term working standard. In this calibration method multiple (ten) samples of each of the short term and the long-term working standards were measured and the former working standard was quantified. During data acquisition, the working standard and air samples were alternatively introduced into the system (a total of 12 data points were acquired in every 24 hour cycle). The data acquisition frequency and procedure maintain a high precision by minimising instrument drift in the Agilent MSD response. The system precision varied for the different compounds. The following precisions were determined from the residual standard deviation of repeated standard samples analysed (Table 1).

The variability in the standards can be driven by a number of factors including elevated blanks, carryover from extreme samples and bleed from the Nafion membrane, in addition to normal instrumental detection variability. Elevated mixing ratios in the blank samples could indicate that there is contamination in the system through either the carrier gas or a leak in the system. Some of the compounds of interest might remain on the trap during desorption, particularly when elevated mixing ratios are sampled. This can lead to carryover on the trap, resulting in a skewed performance of the system. As a precaution against carryover, the trap was repeatedly heated to 240 ºC prior to the trapping of the subsequent sample. An assessment of the system suggests that neither carryover nor a leak into the system occurs here. The Nafion membrane, counter purged with dry nitrogen, was used to dry samples prior to trapping on the adsorbent bed. This permeable membrane, concentrically housed in an exterior tube containing the dry counter-purge gas, allows water to be drawn out of the air without affecting the mixing ratio of the compounds of interest in the sample. Although there is growing concern that the Nafion membrane may adsorb some compounds, particularly bromoform, and then desorb them

later (O'Doherty/Yokouchi pers. coms.). We have seen no direct evidence of Nafion bleed at Cape Point, and the precision of bromoform analysis relative to other species would seem to indicate that the effect, if present, is minimal.

2.3. Air mass characterisation

Complimentary meteorological and radon (^{222}Rn) data from the GAW station supported the analysis of the halocarbon measurements reported here (Labuschagne et al., 2018). Air masses arriving at Cape Point were categorised based on both wind direction and ^{222}Rn concentration (Brunke et al., 2004; Botha et al., 2018). Baseline clean air mass conditions at Cape Point, free from anthropogenic pollution, were defined as air masses arriving from a sectorial wind direction of 120º - 320º and with ^{222}Rn concentrations of < 350 mBq m^{-3} (Brunke et al., 2004). Further characterisation of arriving air masses was done using ^{222}Rn concentrations with anthropogenically modified air defined with a ^{222}Rn concentration of 1000-1500 mBq m^{-3} and continental air as defined as having a ^{222}Rn concentration of >2000 mBq m^{-3} (Brunke et al., 2004; Botha et al., 2018). A further category of ultra clean air masses is defined as air masses arriving from a sectorial wind direction of 170º - 320º and with ^{222}Rn concentrations of < 100 mBq m^{-3} (Brunke, Personal Communications). The data were sorted following the air mass characterisation techniques described above.

HySPLIT back trajectories (https://www.ready.noaa.gov/HYSPLIT.php) were generated every two hours for the duration of the data collected in 2017 (Stein et al., 2015). National Centres for Environmental Prediction (NCEP) re-analysis meteorological data was used to generate the back trajectories. Each trajectory was calculated for 96 hours from the point of origin, Cape Point. The halocarbon measurements were paired with the relevant back trajectory. The R package "openair" was used to calculate the concentration weighted trajectories (CWT) (Carslaw and Ropkins, 2012). This calculation was applied to the halocarbon measurements at Cape Point to examine possible source regions (Carslaw and Ropkins, 2012). The CWT algorithm calculates the number of trajectories, which have an elevated mixing ratio, that pass through the same latitude and longitude position. If a large number of the trajectories (with elevated mixing ratios) pass through a particular point, then the likelihood increases that this point is a source region.

3. Results and Discussion

3.1 Time series of observations

The CH_3I, $CHBr_3$, CH_2Br_2, and CH_3Br mixing ratio datasets for Cape Point between January and November 2017 are presented in Figure 2. The datasets were split into two periods: late austral summer/autumn (Sum-Aut: January-May) and austral winter/spring (Win-Spr: June-November). The missing data, due to instrumental maintenance in May/June, separates the two sampling periods. Occasional increases of short-lived halocarbon mixing ratios were observed (Fig. 2). Supporting meteorological data and ^{222}Rn observations indicated that some of these increases, particularly in March, and at the end of May and again at the end of July, were primarily due to the arrival of anthropogenically modified air from the greater Cape Town region. The remainder of the halocarbon mixing ratio increases, were most likely wind direction change driven variations reflecting different trace gas sources. The mean background atmospheric mixing ratios were comparable with each other for all the species with the exception of CH_3Br, which was higher in the Cape Town air (Table 2). This observation suggests that there may be a significant contribution of terrestrial, biogenic and anthropogenic sources of CH_3Br measured at Cape Point. Variations in the sources over the two seasonal windows and a comparison of background and city air masses are discussed later.

The seasonal mean atmospheric mixing ratio for $CHBr_3$ was higher in the austral Win-Spr (Jul-Nov) than the austral Sum-Aut (Jan-May). Conversely, the mixing ratio of CH_3I was lower in the austral Win-Spr months and higher in the austral Sum-Aut months. These seasonal differences were confirmed to be statistically different using the Welch two sample t-test, *viz* CH_3I ($t = 32.39$, degrees of freedom (DF) = 230, $p = 2.2 \times 10^{-16}$) and $CHBr_3$ ($t = 8.39$, DF = 826, $p = 2.2 \times 10^{-16}$). For CH_3I and $CHBr_3$, this result suggests a local seasonal cycle. Interestingly the CH_2Br_2 and CH_3Br mixing ratios were comparable across the two seasonal windows (Table 2), *viz* CH_2Br_2 ($t = 1.08$, DF = 739, $p = 0.27$) and CH_3Br ($t = 1.25$, DF = 799, $p = 0.21$). Consistent sources, independent of the season may play an active role in the similar mixing ratios for CH_2Br_2 and CH_3Br observed here (Table 2).

When the data were sorted for different air mass types, the air mass attributed to the city of Cape Town displayed a mean CH_3Br mixing ratio that was deemed to be different (statistically significant where $t= 5.85$, DF = 78, $p = 1.04 \times 10^{-7}$) to the mean mixing ratio of CH_3Br in the

clean marine air (Table 2). This observation is not unexpected given the various anthropogenic and terrestrial sources of CH_3Br discussed previously. The CH_3I, $CHBr_3$ and CH_2Br_2 mixing ratios remained largely consistent between the Cape Town (0.64 ± 0.33, 2.02 ± 0.88, 1.10 ± 0.18 ppt, respectively) and the clean marine (0.61 ± 0.29, 2.02 ± 0.78, 1.08 ± 0.17 ppt, respectively) air masses suggesting the ocean is the main source of these compounds.

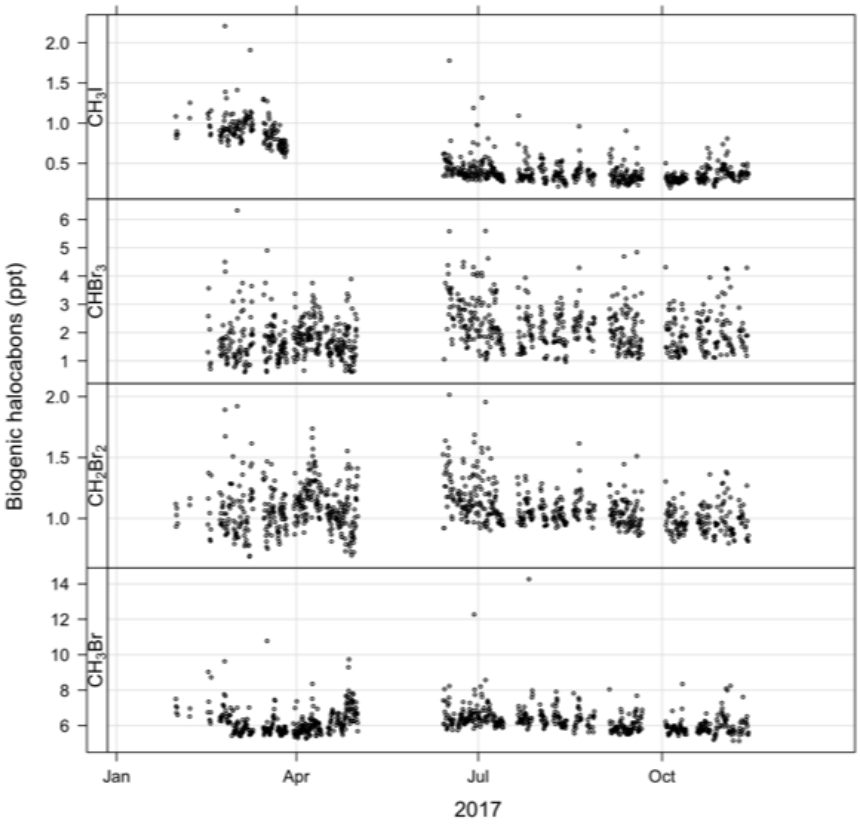

Fig. 2. Time series of biogenic halocarbons measured at Cape Point from January (austral summer) to November (austral spring) 2017. Note: The data missing from May to June 2017 due to the instrumental maintenance.

Table 2. Short-lived volatile organic halocarbon measurements (ppt) at Cape Point under different time and meteorological regimes and their comparison with other southern hemispheric measurement data.

	Conditions		CH_3I	$CHBr_3$	CH_2Br_2	CH_3Br	Ref
Background	120º > WD < 320º & ^{222}Rn < 350 mBq m^{-3}	Mean (sd)	0.61 (0.29) n = 125	2.02 (0.89) n = 150	1.08 (0.17) n = 163	6.09 (0.50) n = 155	1
		Min-max	0.21-1.41	0.60-6.32	0.70-1.92	5.27-8.72	1
Cape Town	120º < WD > 320º & ^{222}Rn > 1500 mBq m^{-3}	Mean (sd)	0.64 (0.33) n = 150	2.02 (0.78) n =184	1.10 (0.18) n = 188	6.44 (0.74) n = 179	1
		Min-max	0.26-2.21	0.61-4.84	0.69-1.90	5.40-9.63	1
Sum-Aut (all)	Jan – Jun	Mean (sd)	0.93 (0.25) n =	1.75 (073) n = 369	1.08 (0.19) n =	6.18 (0.73) n =	1

			175		387	377	
		Min-max	0.58-3.07	0.60-6.32	0.69-1.92	5.27-10.75	1
Win-Spr (all)	Jul - Dec	Mean (sd)	0.39 (0.17) n = 547	2.18 (0.79) n = 515	1.07 (0.16) n = 547	6.25 (0.71) n = 535	1
		Min-max	0.20-2.72	0.97-5.60	0.80-2.04	5.13-14.26	1
Cape Point	Oct-Nov 2011	Mean (sd)		24.8 (14.8)			2
		Min-max		4.4-64.6			2
San Cristobol Island (0.92° S)	Feb-Mar 2002-2003	Mean (sd)		14.2 (10.1)	3.2(1.5)		3
		Min-max		4.2-43.6	1.8-7.6		3
Peruvian upwelling (5-16° S)	Dec 2012	Mean	1.6	2.9	1.3		4
		Min-max	0.6-3.2	1.5-5.9	0.8-.2.0		4
SW Indian Ocean (2-30° S)	Jun – Aug 2014	Mean (sd)	0.84 (0.12)	1.20 (0.35)	0.91 (0.08)	-	5
		Min-max	0.57-1.22	0.68-2.97	0.77-1.20	-	5
RV Hakshuo (15-44° S)	Dec 1996 – Feb 1997	Mean (sd)	1.1(0.4)			8.6(0.6)	6
RV Shirase (15-44° S)	Dec 1996-Feb 1997	Mean (sd)				8.2(1.1)	6
Cape Grim (40.7^{O} S)	Jan-Feb 1999	Mean	2.6	2.6	0.43		7
		Min-Max	1.0-7.3	0.7-8.0	0.10-1.39		
Cape Grim (40.7^{O} S)	2003	Mean (sd)		2.9(1.2)	1.1(0.2)		3
		Min-max		1.3-6.4	0.7-1.7		3
Coastal South America (55^{O} S)	Dec 2007-Jan 2008	Mean(sd)		7.4(3.0)			8
		Min-max		1.8-11			8
Southern Ocean	1994-2004	Mean	0.6	1.0	0.9		9
		Range	0.2-1.1	0.4-2.1	0.6-1.3		
Antarctic Coast (65° S)	Dec 2007-Jan 2008	Mean(sd)		3.2(0.7)			8
		Min-max		2.1-4.9			8
Antarctic Ocean (65-67° S)	Dec 2007-Jan 2008	Mean(sd)		2.3(0.4)			8
		Min-max	2.4(21.5)	1.9-3.9			8
Antarctic Coast (60-66° S)	Oct-Dec 1987	Mean(sd)					10

Ref: 1. This study; 2. Kuyper et al. (2018); 3. Yokuchi et al. (2005); 4. Hepach et al. (2016); 5. Fiehn et al. (2017); 6. Li et al. (2001); 7. Carpenter et al. (2003); 8. Mattsson et al., (2013); 9. Butler et al. (2007); 10. Reifenhauser and Heumann (1992)

Figure 3 shows the 'openair' concentration weighted trajectory analysis for each of the four compounds showing their likely origin (Carslaw and Ropkins, 2012). The difference in the fetch of the trajectories between Sum-Aut and Win-Spr, which stretches as far south as Antarctica in the Win-Spr could be related to changes in the synoptic climatology (Tyson and Preston-Whyte, 2000). The Sum-Aut period is dominated by strong south-easterly winds driven by the anti-

clockwise South Atlantic High Pressure (SAHP). The majority of the sources of halocarbons measured at Cape Point for both seasonal periods appears to originate from the south Atlantic Ocean, north of the Antarctic Polar Front (APF: 50 ºS, Fig. 3). A visual inspection of Figures 3a and 3b suggest that there is a significant difference in the sources of CH_3I during the Sum-Aut and Win-Spr periods. This difference may reflect either increased planktonic or photochemical production of CH_3I in the south Atlantic ocean during the Sum-Aut period (Moore and Zafiriou, 1994; Ooki et al., 2015). Given the extensive biomass of subtidal kelp along the South African coast, Figure 3c indicates that there is, not unexpectedly, a persistent coastal contribution of $CHBr_3$. Further a second source of $CHBr_3$, particularly in the Win-Spr months, may be pelagic and aligned with the APF (Fig. 3d). Despite the strong SE wind regime found during the Sum-Aut months, CH_2Br_2 and CH_3Br displayed a maximum mean mixing ratio from the north-west (Fig. 3e and 3h). This may be a contribution from extensive endemic vegetation (fynbos) fires on the mountain ranges of the Western Cape and veldfires in the interior of South Africa.

The halocarbon observations reported here are of significance as this region of the global oceans is characterised by a paucity of both oceanic and atmospheric halocarbon data (Ziska et al., 2013). Interestingly, there has been a single study of the seawater concentrations of the same suite of compounds (Abrahamsson et al., 2004) along the Good Hope transect line from Cape Town to Antarctica, between 18 ºE and 5 ºW. Ziska et al. (2013) estimated regional sea-air fluxes for CH_3I, $CHBr_3$ and CH_2Br_2 from a global set of seawater and air measurements. The estimated flux strengths for $CHBr_3$ is weak in the south Atlantic and negative (representing an oceanic $CHBr_3$ sink) in the Southern Ocean (Ziska et al., 2013). The approximate position of the APF appears to straddle these two regions. The estimated fluxes for CH_3I and CH_2Br_2 are positive through the south Atlantic and Southern Ocean. The estimated CH_3I sea-air flux, while moderate throughout the south Atlantic, decreases in strength south of the APF. A weak CH_2Br_2 flux strength in the south Atlantic is contrasted with a stronger flux for this gas south of APF (Ziska et al., 2013). The positive or negative direction of the CH_3Br sea-air flux depends on the saturation state of the seawater (Hu et al., 2010). Given the estimated flux strengths and directions of Ziska et al. (2013) and Hu et al. (2010), it would be reasonable to use the study by Abrahamsson et al. (2004) as an approximation of location of possible source regions of these compounds. However, the results reported from this study are at variance with the observations recorded by Abrahamsson et al. (2004), with mixing ratios of brominated and iodinated

compounds decreasing between the sub-tropical front (STF) and the APF. Abrahamsson et al. (2004) also observed an increase in brominated compound concentrations at, and south of, the APF, particularly for $CHBr_3$. The physics and dynamics of these ocean fronts have been studied since their discovery in the 1930s (Belkin and Gordon, 1996). Local physical and thermodynamic processes play a pivotal role in the strength and position of the frontal boundaries in the Southern Ocean (e.g. Belkin and Gordon, 1996; Froneman et al., 2007). Furthermore, the Southern Ocean is regarded as a dynamic environment in which there is spatial and temporal mesoscale variability in temperature, salinity and biomass (Froneman et al., 2007).

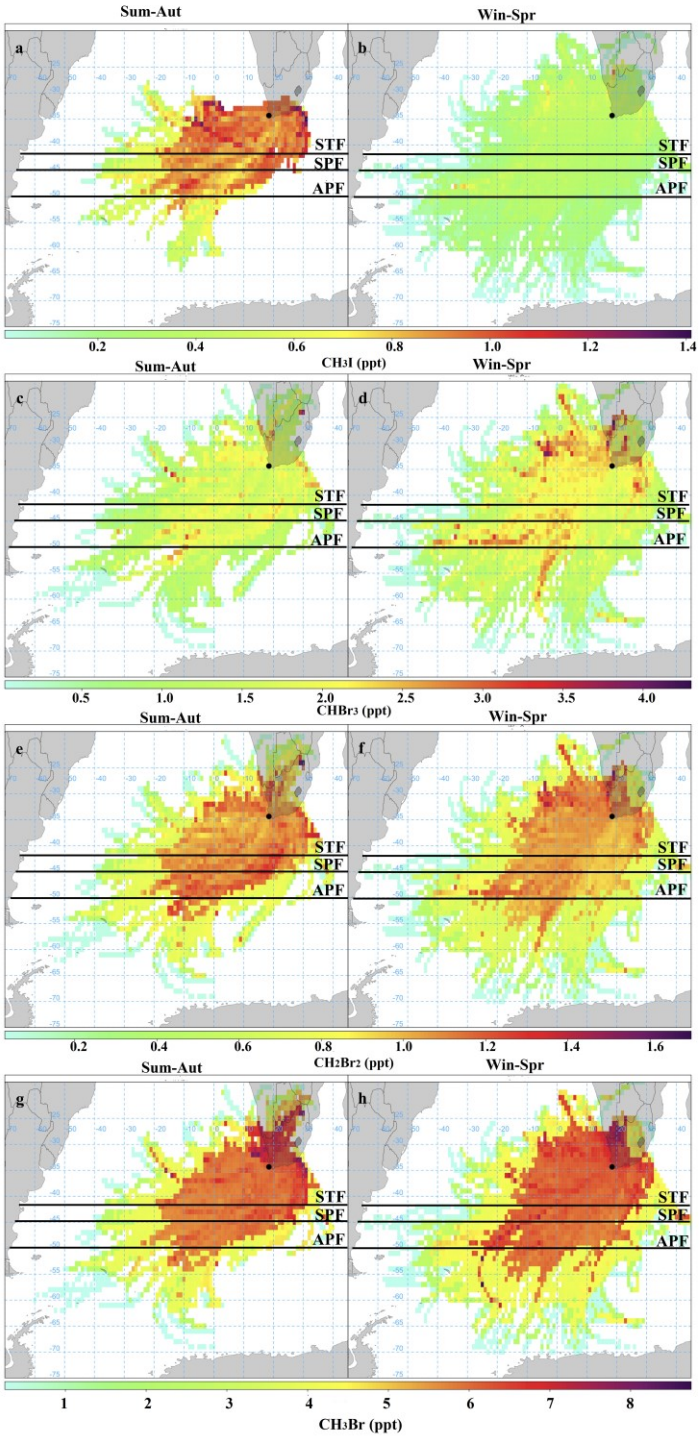

Fig. 3. Concentration Weighted Trajectory (CWT) calculated possible source origins calculated for the austral Sum-Aut and the austral Win-Spr for: a-b) methyl iodide, c-d) bromoform, e-f) dibromomethane and g-h) methyl bromide arriving at Cape Point. The sub-tropical front (STF), sub-Antarctic Front (SAF) and Antarctic Polar Front (APF) are indicated. Cape Point GAW station shown by black point.

3.2. Comparison with other studies

There is one previous set of measurements of $CHBr_3$ taken at the Cape Point observatory (Kuyper at al., 2018) from October to November 2011 that reports levels ranging from approximately 4 – 64 ppt with a mean value of 24.8 ppt. These data are quite a bit larger than the much longer time-series established here, i.e. a mean value of 2.02 ± 0.89 ppt and a range of approximately 1- 5 ppt. It is impossible to cross calibrate the two studies given the difference in time between the two (no standard available from the 2011 study) and so the possibility of calibration differences cannot be ruled out. However, assuming that instrumental, detection and calibration differences do not bias a comparison, the data from Kuyper et al. (2018) are high in comparison with other Southern Hemisphere studies (see Table 2) and this study is consistent with other data from the Southern Hemisphere. Given the transitory nature of natural sources, it is perfectly possible for high levels of $CHBr_3$ to have been observed by Kuyper et al. (2018) in 2011 but this current study is likely to be more representative of the mean levels and their variability at Cape Point.

Inspection of Table 2 shows that in general, levels measured at Cape Point for CH_3I, $CHBr_3$ and CH_2Br_2 are comparable with other southern hemisphere measurements. It is well known that CH_3Br levels have been declining globally (e.g. Carpenter and Reimann, 2014) and so measurements made in 1997 (see Table 2) are expected to be larger. Data reported by Hossaini et al. (2013) show that there is a seasonal cycle for $CHBr_3$ at the Cape Grim Observatory, peaking in February, whereas a similar cycle is not observed at Cape Point, although similar levels are reported in both studies. In addition, a weak seasonal cycle for CH_2Br_2 (around 1 ppt average) peaking in winter is reported which is consistent with data in this study. The global model study of CH_3I by Bell et al. (2002) suggests good agreement with this study in terms of seasonality and magnitude.

3.3 Relationship between CH_2Br_2 and $CHBr_3$ mixing ratios

The ratio $\ln([CH_2Br_2]/[CHBr_3]):\ln([CHBr_3])$, increases with transport from sources due to the higher degradation rate of $CHBr_3$ relative to CH_2Br_2 (Yokouchi et al., 2017). In an atmosphere with minimal mixing, a chemical decay line is calculated using the cleanest marine air (Rn < 100

mBq m^{-3}) at Cape Point as follows as outlined by Yokouchi et al. (2017).

$$\ln([CH_2Br_2]/[CHBr_3]) = (k_{CH_2Br_2}/k_{CHBr_3} - 1) \cdot \ln([CHBr_3]) + \ln([CH_2Br_2]_0) - k_{CH_2Br_2}/k_{CHBr_3} \cdot \ln([CHBr_3]_0) \quad [1]$$

Where $[CHBr_3]_0$ and $[CH_2Br_2]_0$ represent the initial concentrations and $[CHBr_3]$ and $[CH_2Br_2]$ represent the final concentrations of $CHBr_3$, and CH_2Br_2, respectively. k_{CHBr_3} and $k_{CH_2Br_2}$ are the pseudo first order rate constants for the decay of $CHBr_3$, and CH_2Br_2 which were calculated using their lifetimes of 123 days and 24 days, respectively (Montzka and Reimann, 2011; Yokouchi et al., 2017). The gradient ($[CH_2Br_2]/[CHBr_3]$-1) and intercept of the decay line ($\ln([CH_2Br_2]_0) - k_{CH_2Br_2}/k_{CHBr_3} \cdot \ln([CHBr_3]_0)$), are determined to be -0.72 and -0.07, respectively. Thu the chemical decay line at Cape Point can be defined in aged air by the following equation:

$$\ln([CH_2Br_2]/[CHBr_3]) = -0.72 \cdot \ln([CHBr_3]) - 0.07 \quad [2]$$

Deviations from the general decay rate suggests either variations in the source strength or atmospheric mixing (dilution). According to Yokouchi et al. (2017), the mixing or dilution of $CHBr_3$ and CH_2Br_2 in the atmosphere would cause a slight shift to the left of the chemical decay line, while a shift to the right of the chemical decay line suggests higher $[CHBr_3]$:$[CH_2Br_2]$ ratios in sources. In this study, across the entire times series the $\ln([CH_2Br_2]/[CHBr_3])$:$\ln([CHBr_3])$ ratio for Cape Point is shifted to the right of the general chemical decay line, represented by the dashed line in Figure 4a. The linear regression of the entire time series, with a gradient of -0.67, suggests greater $[CHBr_3]$:$[CH_2Br_2]$ ratios in the local sources at Cape Point. Seasonal analysis of the $\ln([CH_2Br_2]/[CHBr_3])$:$\ln([CHBr_3])$ ratio suggests slightly greater $[CHBr_3]$:$[CH_2Br_2]$ source ratios in Sum-Aut (gradient -0.61; Figure 4c), compared with Win-Spr (gradient -0.66; Figure 4b). Given that the lifetime of bromoform will decrease relative to dibromomethane in the summer, the increase in the ratio is evidence of a non-negligible increase in bromoform emissions compared with dibromomethane for the summer-autumn period. Increased local marine bioactivity but also local biogenic terrestrial sources could well explain this increase. The strong southerly winds that dominate through the austral Sum-Aut months most likely result in

increased emission fluxes from the extensive kelp beds surrounding Cape Point. The back trajectory analysis suggests that the higher mixing ratios are closer to shore. During the austral Win-Spr months north-westerly winds dominate, which draws air from over the kelp beds to the north of Cape Point, allowing the ageing of the air mass and this results in a gradient that more closely matches the general decay line. Overall the ln([CH_2Br_2]/[$CHBr_3$]):ln([$CHBr_3$]) ratio calculated from the Cape Point data, both over the entire times series and with seasonal differentiation, compares favourably with the ratios reported by Yokouchi et al. (2017).

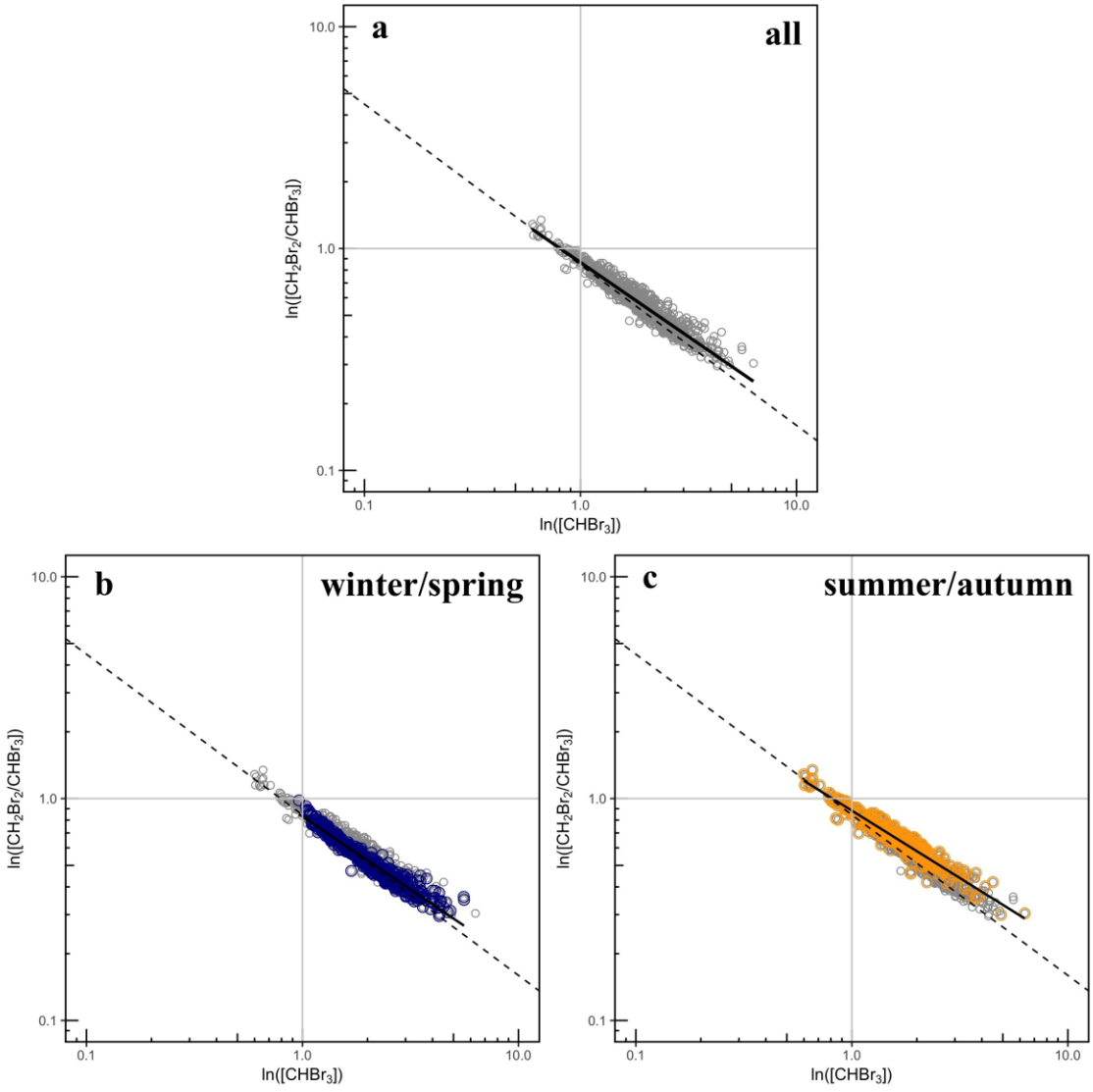

Fig. 4. Relationship between ln([CH_2Br_2/$CHBr_3$]) and ln[$CHBr_3$] in air samples collected from Cape Point. (a) All data shown (grey circles). (b) austral Win-Spr (blue circles), (c) austral Sum-Aut (orange circles). Note: All data are also shown in Figure b and c as grey circles. Dashed lines shows the general decay lines with a gradient of -0.72 and intercept of -0.07. Regression of the

relative data shown by the solid line.

4. Conclusion

The data presented here represents the first CH_3I, CH_3Br, CH_2Br_2, and $CHBr_3$, data series for two extended time periods (Sum-Aut and Win-Spr) from a southern African marine environment. The mean baseline atmospheric mixing ratios for CH_3I, $CHBr_3$, CH_2Br_2 and CH_3Br at Cape Point from combining both time period data series were established as 0.61 ± 0.29, 2.02 ± 0.89, 1.08 ± 0.18 and 6.09 ± 0.50 ppt, respectively. While the mixing ratios of CH_2Br_2 and CH_3Br showed no seasonal variation, a higher mixing ratio of $CHBr_3$ and a lower mixing ratio of CH_3I, were observed during the austral Win-Spr months. Concentration-weighted trajectory (CWT) analyses indicated that the Southern Ocean is a significant source of these halocarbons. Only the source of CH_3I showed a strong seasonal variation. An analysis of the $\ln([CH_2Br_2]/[CHBr_3]):\ln([CHBr_3])$ ratio would suggest that there are greater atmospheric $[CHBr_3]:[CH_2Br_2]$ source ratios in air masses arriving at Cape Point during the austral Sum-Aut months compared with austral Win-Spr. This study underlines the importance of the Cape Point GAW station in increasing our understanding of the contribution of the Southern Ocean to volatile halocarbon concentrations in the atmosphere above the southern Africa.

Acknowledgements

The authors would like to thank the Atmospheric Chemistry Research Group at the University of Bristol, UK for their continued support and advice. The authors would like to thank Gerry Spain at Mace Head for his help with filing the standard tank and the analysing of it. James Matthew for sourcing and shipping parts as needed. Paul Keanly for his efforts in rebuilding a critical component from scratch. The authors would like to thank the following grants for making this research possible: NE/P013104, NE/K01501X, and Bristol ChemLabs under whose auspices Outreach associated with this work was carried out. DES would like to thank UWC for an extraordinary Professorship.

References

Abrahamsson, K., Bertilsson, S., Chierici, M., Fransson, A., Froneman, P.W., Lorén, A., Pakhomov, E.A., 2004. Variations of biochemical parameters along a transect in the Southern Ocean, with special emphasis on volatile halogenated organic compounds. Deep. Res. Part II Top. Stud. Oceanogr. 51, 2745–2756.

Anderson, R., Rand, A., Rothman, M., Share, A., Bolton, J.J., 2007. Mapping and quantifying the South African kelp resource. African J. Mar. Sci. 29, 369–378.

Arnold, T., Mühle, J., Salameh, P.K., Harth, C.M., Ivy, D.J., Weiss, R.F., 2012. Automated

Measurement of Nitrogen Trifluoride in Ambient Air. Anal. Chem. 84, 4798–4804.
Aschmann, J., Sinnhuber, B.M., 2013. Contribution of very short-lived substances to stratospheric bromine loading: Uncertainties and constraints. Atmos. Chem. Phys. 13, 1203–1219.
Ashfold, M.J., Harris, N.R.P., Manning, A.J., Robinson, A.D., Warwick, N.J., Pyle, J.A., 2014. Estimates of tropical bromoform emissions using an inversion method. Atmos. Chem. Phys. 14, 979–994.
Belkin, I.M., Gordon, A.L., 1996. Southern Ocean fronts from the Greenwich meridian to Tasmania. J. Geophys. Res. C Ocean. 101, 3675–3696. https://doi.org/10.1029/95JC02750
Bell, N., Hsu, L., Jacob, D.J., Schultz, M.G., Blake, D.R., Butler, J.H., King, D.B., Lobert, J.M., Maier-Reimer, E., 2002. Methyl iodide: Atmospheric budget and use as a tracer of marine convection in global models. J. Geophys. Res. Atmos. 107, 4340.
Bloss, W.J., Lee, J.D., Johnson, G.P., Sommariva, R., Heard, D.E., Saiz-Lopez, A., Plane, J.M.C., McFiggans, G.B., Coe, H., Flynn, M.J., Williams, P., Rickard, A., Fleming, Z.L., 2005. Impact of halogen monoxide chemistry upon boundary layer OH and HO_2 concentrations at a coastal site. Geophys. Res. Lett. 32, 1–4.
Botha, R., Labuschagne, C., Williams, A.G., Bosman, G., Brunke, E., Rossouw, A., Lindsay, R., 2018. Characterising fifteen years of continuous atmospheric radon activity observations at Cape Point (South Africa). Atmos. Environ. 176, 30–39.
Bravo-Linares, C.M., Mudge, S.M., Loyola-Sepulveda, R.H., 2010. Production of Volatile Organic Compounds (VOCs) By Temperate Macroalgae: the Use of Solid Phase Microextraction (SPME) Coupled To GC-MS As Method of Analysis. J. Chil. Chem. Soc. 55, 227–232.
Brownell, D.K., Moore, R.M., Cullen, J.J., 2010. Production of methyl halides by prochlorococcus and synechococcus. Global Biogeochem. Cycles 24, 1–7.
Brunke, E., Halliday, E.C., 1983. Halocarbon measurements in the southern hemisphere since 1977. Atmos. Environ. 17, 823–826.
Brunke, E., Labuschagne, C., Parker, B., Scheel, H.E., Whittlestone, S., 2004. Baseline air mass selection at Cape Point, South Africa: Application of ^{222}Rn and other filter criteria to CO_2. Atmos. Environ. 38, 5693–5702.
Brunke, E., Walters, C., Mkololo, T., Martin, L.G., Labuschagne, C., Silwana, B., Slemr, F., Weigelt, A., Ebinghaus, R., Somerset, V., 2016. Mercury in the atmosphere and in rainwater at Cape Point, South Africa. Atmos. Environ. 125, 24–32.
Butler, J.H., 1995. Methyl bromide under scrutiny. Nature 376, 469–470.
Butler, J.H., King, D.B., Lobert, J.M., Montzka, S.A., Yvon-Lewis, S.A., Hall, B.D., Warwick, N.J., Mondeel, D.J., Aydin, M., Elkins, J.W., 2007. Oceanic distribution and emissions of short-lived halocarbons. Global Biogeochem. Cycles 21, GB1023.
Carpenter, L.J., 2003. Iodine in the Marine Boundary Layer. Chem. Rev. 103, 4953–4962.
Carpenter, L.J., Jones, C.E., Dunk, R.M., Hornsby, K.E., Woeltjen, J., 2009. Air-sea fluxes of bromine from the tropical and North Atlantic Ocean. Atmos. Chem. Phys. 9, 1805–1816.
Carpenter, L.J., Liss, P.S., 2000. On temperate sources of bromoform and other reactive organic bromine gases. J. Geophys. Res. 105, 20539–20547.
Carpenter, L.J., Malin, G., Liss, P.S., Küpper, F.C., 2000. Novel biogenic iodine-containing trihalomethanes and other short-lived halocarbons in the coastal East Atlantic. Global Biogeochem. Cycles 14, 1191–1204.
Carpenter, L.J., Liss, P.S., Penkett, S.A., 2003. Marine organohalogens in the atmosphere over

the Atlantic and southern Oceans. J. Geophys. Res. Atmos. 108, 4256.
Carpenter, L.J., Nightingale, P.D., 2015. Chemistry and Release of Gases from the Surface Ocean. Chem. Rev. 115, 4015–4034.
Carpenter, L.J., Reimann, S., 2014. Update on Ozone-Depleting Substances (ODSs) and Other Gases of Interest to the Montreal Protocol, in: Scientific Assessment of Ozone Depletion: 2014. World Meteorological Organization, Geniva, Swizerland, pp. 1–105.
Carpenter, L.J., Sturges, W.T., Penkett, S.A., Liss, P.S., Alicke, B., Hebestreit, K., Platt, U., 1999. Short-lived alkyl iodides and bromides at Mace Head, Ireland: Links to biogenic sources and halogen oxide production. J. Geophys. Res. 104, 1679–1689.
Carslaw, D.C., Ropkins, K., 2012. Openair - An R package for air quality data analysis. Environ. Model. Softw. 27–28, 52–61.
Fiehn, A., Quack, B., Hepach, H., Fuhlbrügge, S., Tegtmeier, S., Toohey, M., Atlas, E.L., Krüger, K., 2017. Delivery of halogenated very short-lived substances from the West Indian Ocean to the stratosphere during Asian summer monsoon. Atmos. Chem. Phys. Discuss. 1–40.
Fraser, P.J., Oram, D.E., Reeves, C.E., Penkett, S.A., McCulloch, A., 1999. Southern hemispheric halon trends (1978-1998) and global halon emissions. J. Geophys. Res. 104, 15985–15999.
Froneman, P.W., Ansorge, I.J., Richoux, N., Blake, J., Daly, R., Sterley, J., Mostert, B., Heyns, E., Sheppard, J., Kuyper, B., Hart, N., George, C., Howard, J., Mustafa, E., Pey, F., Lutjeharms, J.R.E., 2007. Physical and biological processes at the Subtropical Convergence in the South-west Indian Ocean. S. Afr. J. Sci. 103, 193–195.
Fuhlbrügge, S., Quack, B., Tegtmeier, S., Atlas, E., Hepach, H., Shi, Q., Raimund, S., Krüger, K., 2016. The contribution of oceanic halocarbons to marine and free tropospheric air over the tropical West Pacific. Atmos. Chem. Phys. 16, 7569–7585.
Garstang, M., Tyson, P.D., Edwards, M., Kallberg, P., Lindesay, J.A., 1996. Horizontal and vertical transport of air over southern Africa. J. Geophys. Res. 101, 23721–23736.
Giese, B., Latumus, F., Adams, F.C., Wiencke, C., 1999. Release of Volatile Iodinated C_1−C_4 Hydrocarbons by Marine Macroalgae from Various Climate Zones. Environ. Sci. Technol. 33, 2432–2439.
Ginger, T., Hasan, O., Sandler, S.I., 1992. Infinite Dilution Activity Coefficients and Henry's Law Coefficients of Some Priority Water Pollutants Determined by a Relative Gas Chromatographic Method. Environ. Sci. Technol. 26, 2017–2022.
Goodwin, K.D., 1996. Natural cycles of brominated methanes: Macroalgal production and marine microbial degradation of bromoform and dibromomethane. PhD Thesis, California Institute of Technology, USA
Goodwin, K.D., North, W.J., Lidstrom, M.E., 1997. Production of bromoform and dibromomethane by Giant Kelp: Factors affecting release and comparison to anthropogenic bromine sources. Limnol. Oceanogr. 42, 1725–1734.
Happell, J.D., Wallace, D.W.R., 1996. Methyl iodide in the Greenland/Norwegian Seas and the tropical Atlantic Ocean: Evidence for photochemical production. Geophys. Res. Lett. 23, 2105–2108.
Happell, J.D., Wallace, D.W.R., Wills, K.D., Wilke, R.J., Neill, C.C., 1996. A purge-and-trap capillary column gas chromatographic method for the measurement of halocarbons in water and air, Report. ed. Brookhaven National Laboratory, Upton, N.Y.
Hepach, H., Quack, B., Tegtmeier, S., Engel, A., Bracher, A., Fuhlbrügge, S., Galgani, L., Atlas,

E.L., Lampel, J., Frieβ, U., Krüger, K., 2016. Biogenic halocarbons from the Peruvian upwelling region as tropospheric halogen source. Atmos. Chem. Phys. 16, 12219–12237.
Hossaini, R., Chipperfield, M.P., Monge-Sanz, B.M., Richards, N.A.D., Atlas, E., Blake, D.R., 2010. Bromoform and dibromomethane in the tropics: a 3-D model study of chemistry and transport. Atmos. Chem. Phys. 10, 719–735.
Hossaini, R., Chipperfield, M.P., Montzka, S.A., Rap, A., Dhomse, S.S., Feng, W., 2015. Efficiency of short-lived halogens at influencing climate through depletion of stratospheric ozone. Nat. Geosci. 8, 186–190.
Hossaini, R., Mantle, H., Chipperfield, M.P., Montzka, S.A., Hamer, P.D., Ziska, F., Quack, B., Krüger, K., Tegtmeier, S., Atlas, E.L., Sala, S., Engel, A., Bönisch, H., Keber, T., Oram, D., Mills, G., Ordonez, C., Saiz-Lopez, A., Warwick, N.J., Liang, Q., Feng, W., Moore, F., Miller, B.R., Marécal, V., Richards, N.A.D., Dorf, M., Pfeilsticker, K., 2013. Evaluating global emission inventories of biogenic bromocarbons. Atmos. Chem. Phys. 13, 11819–11838.
Hu, L., Yvon-lewis, S.A., Liu, Y., Salisbury, J.E., O'Hern, J.E., 2010. Coastal emissions of methyl bromide and methyl chloride along the eastern Gulf of Mexico and the east coast of the United States. Global Biogeochem. Cycles 24, GB1007.
Jones, C.E., Hornsby, K.E., Dunk, R.M., Leigh, R.J., Carpenter, L.J., 2009. Coastal measurements of short-lived reactive iodocarbons and bromocarbons at Roscoff, Brittany during the RHaMBLe campaign. Atmos. Chem. Phys. 9, 8757–8769.
Khalil, M.A.K., Rasmussen, R.A., Gunawardena, R., 1993. Atmospheric Methyl Bromide : Trends and Global Mass Balance. J. Geophys. Res. 98, 2887–2896.
Krüger, K., Quack, B., 2013. Introduction to special issue: The *TransBrom Sonne* expedition in the tropical West Pacific. Atmos. Chem. Phys. 13, 9439–9446.
Kuyper, B., Palmer, C.J., Labuschagne, C., Reason, C.J.C., 2018. Atmospheric bromoform at Cape Point, South Africa: a first time series on the African continent. Atmos. Chem. Phys. 18, 5785–5797.
Labuschagne, C., Kuyper, B., Brunke, E., Spuy, D. Van Der, Martin, L., Mbambalala, E., Khan, M.A.H., Davies-coleman, M.T., Shallcross, D.E., Joubert, W., 2018. A review of four decades of atmospheric trace gas measurements at Cape Point, South Africa. Trans. R. Soc. South Africa 1–20.
Li, H.J., Yokouchi, Y., Akimoto, H., Narita, Y., 2001. Distribution of methyl chloride, methyl bromide, and methyl iodide in the marine boundary air over the western Pacific and southeastern Indian Ocean. Geochem. J. 35, 137–144.
Lee-Taylor, J.M., Holland, E.A., 2000. Litter decomposition as a potential natural source of methyl bromide. J. Geophys. Res. Atmos. 105, 8857–8864.
Louw, D.C., Plas, A.K. Van Der, Mohrholz, V., Wasmund, N., Junker, T., Eggert, A., 2016. Seasonal and interannual phytoplankton dynamics and forcing mechanisms in the Northern Benguela upwelling system. J. Mar. Syst. 157, 124–134.
Manley, S.L., Dastoor, M.N., 1987. Methyl halide (CH_3X) production from the giant kelp, *Macrocystis*, and estimates of global CH_3X production by kelp. Limnol. Oceanogr. 32, 709–715.
Manley, S.L., Goodwin, K.D., North, W.J., 1992. Laboratory production of bromoform, methylene bromide, and methyl iodide by macroalgae and distribution in nearshore southern California waters. Limnol. Oceanogr. 37, 1652–1659.
Manö, S., Andreae, M.O., 1994. Emission of Methyl Bromide from Biomass Burning. Science

(80-.). 263, 1255–1257.
Mattsson, E., Karlsson, A., and Abrahamsson, K., 2013. Regional sinks of bromoform in the Southern Ocean. Geophys. Res. Lett. 40, 3991–3996.
Miller, B.R., Weiss, R.F., Salameh, P.K., Tanhua, T., Greally, B.R., Mühle, J., Simmonds, P.G., 2008. Medusa: a sample preconcentration and GC-MS detector system for in situ measurements of atmospheric trace halocarbons, hydrocarbons and sulfur compounds. Anal. Chem. 80, 1536–1545.
Montzka, S.A., Reimann, S., 2011. Ozone-depleting Substances (ODSs) and Related Chemicals, in: Scientific Assessment of Ozone Depletion. World Meteorological Organization, pp. 1–108.
Moore, R.M., Zafiriou, O.C., 1994. Photochemical production of methyl iodide in seawater. J. Geophys. Res. 99, 16415–16420.
Nightingale, P.D., Malin, G., Liss, P.S., 1995. Production of chloroform and other low-molecular-weight halocarbons by some species of macroalgae. Limnol. Oceanogr. 40, 680–689.
O'Doherty, S.J., Simmonds, P.G., Nickless, G., Betz, W.R., 1993. Evaluation of Carboxen carbon molecular sieves for trapping replacement chlorofluorocarbons. J. Chromatogr. 630, 265–274.
Ooki, A., Nomura, D., Nishino, S., Kikuchi, T., Yokouchi, Y., 2015. A global-scale map of isoprene and volatile organic iodine in surface seawater of the Arctic, Northwest Pacific, Indian, and Southern Oceans. J. Geophys. Res. Ocean. 120, 4108–4128.
Palmer, C.J., Reason, C.J.C., 2009. Relationships of surface bromoform concentrations with mixed layer depth and salinity in the tropical oceans. Global Biogeochem. Cycles 23, 1–10.
Pitcher, G.C., Brown, P.C., Mitchell-Innes, B.A., 1992. Spatio-temporal variability of phytoplankton in the southern Benguela upwelling system. South African J. Mar. Sci. 12, 439–456.
Preston-Whyte, R.A., Tyson, P.D., 1993. The Atmosphere and Weather of Southern Africa. Oxford University Press, Oxford.
Prinn, R.G., Weiss, R.F., Fraser, P.J., Simmonds, P.G., Cunnold, D.M., Alyea, F.N., O'Doherty, S.J., Salameh, P.K., Miller, B.R., Huang, J., Wang, R.H.J., Hartley, D.E., Harth, C.M., Steele, L.P., Sturrock, G.A., Midgley, P.M., McCulloch, A., 2000. A history of chemically and radiatively important gases in air deduced from ALE/GAGE/AGAGE. J. Geophys. Res. 105, 17751.
Quack, B., Suess, E., 1999. Volatile halogenated hydrocarbons over the western Pacific between 43º and 4º N. J. Geophys. Res. 104, 1663–1678.
Quack, B., Wallace, D.W.R., 2003. Air-sea flux of bromoform: Controls, rates, and implications. Global Biogeochem. Cycles 17, 1023.
Read, K.A., Mahajan, A.S., Carpenter, L.J., Evans, M.J., Faria, B.V.E., Heard, D.E., Hopkins, J.R., Lee, J.D., Moller, S.J., Lewis, A.C., Mendez, L., McQuaid, J.B., Oetjen, H., Saiz-Lopez, A., Pilling, M.J., Plane, J.M.C., 2008. Extensive halogen-mediated ozone destruction over the tropical Atlantic Ocean. Nature 453, 1232–1235.
Reeves, C.E., Penkett, S.A., 1993. An estimate of the anthropogenic contribution to atmospheric methyl bromide. Geophys. Res. Lett. 20, 1563–1566.
Reifenhauser, W., Heumann, K.G., 1992. Determinations of methyl iodide in the antarctic atmosphere and the south polar sea. Atmos. Environ. 26, 2905-2912.
Robinson, A.D., Harris, N.R.P., Ashfold, M.J., Gostlow, B., Warwick, N.J., O'Brien, L.M.,

Beardmore, E.J., Nadzir, M.S.M., Phang, S.-M., Samah, A.A., Ong, S., Ung, H.E., Peng, L.K., Yong, S.E., Mohamad, M., Pyle, J.A., 2014. Long-term halocarbon observations from a coastal and an inland site in Sabah, Malaysian Borneo. Atmos. Chem. Phys. 14, 8369–8388.

Sæmundsdóttir, S., Matrai, P., 1998. Biological production of methyl bromide by cultures of marine phytoplankton. Limnol. Oceanogr. 43, 81–87.

Saiz-Lopez, A., Lamarque, J. -F., Kinnison, D.E., Tilmes, S., Ordóñez, C., Orlando, J.J., Conley, A.J.,Plane, M.C., Mahajan, A.S., Santos, G.S., Atlas, E.L., Blake, D.R., Sander, S.P., Schauffler, S., Thompson, A.M., Brasseur, G., 2012. Estimating the climate signicance of halogen-driven ozone loss in the tropical marine troposphere. Atmos. Chem. Phys. 12, 3939–3949.

Sakko, A.L., 1998. The influence of the Benguela upwelling system on Namibia's marine biodiversity. Biodivers. Conserv. 7, 419–433.

Simmonds, P.G., O'Doherty, S.J., Nickless, G., Sturrock, G.A., Swaby, R., Knight, P., Ricketts, J., Woffendin, G., Smith, R., 1995. Automated gas chromatograph/mass spectrometer for routine atmospheric field measurements of the CFC replacement compounds, the hydrofluorocarbons and hydrochlorofluorocarbons. Anal. Chem. 67, 717–723.

Stein, A.F., Draxler, R.R., Rolph, G.D., Stunder, B.J.B., Cohen, M.D., Ngan, F., 2015. NOAA's HYSPLIT atmospheric transport and dispersion modeling system. Bull. Am. Meteorol. Soc. 96, 2059–2077.

Stemmler, I., Hense, I., Quack, B., Maier-Reimer, E., 2014. Methyl iodide production in the open ocean. Biogeosciences 11, 4459–4476.

Sturrock, G.A., Porter, L.W., Fraser, P.J., 2001. In situ measurement of CFC replacement chemicals and other halocarbons at Cape Grim: the AGAGE GC-MS Program, in: Tindale, N.W., Derek, N., Francey, R.J. (Eds.), Baseline 97–98. Bureau of Meteorology, CSIRO, Melbourne, Victoria, pp. 43–49.

Tyson, P.D., Preston-Whyte, R.A., 2000. The Weather and Climate of Southern Africa. Oxford University Press Southern Africa, Cape Town.

Vogt, R., Sander, R., Von Glasow, R., Crutzen, P.J., 1999. Iodine chemistry and its role in halogen activation and ozone loss in the marine boundary layer: A model study. J. Atmos. Chem. 32, 375–395.

WMO, 1995. Scientific Assessment of Ozone Depletion: 1994. World Meteorological Organization, Geniva, Swizerland.

Yang, J.S., 2001. Bromoform in the effluents of a nuclear power plant: A potential tracer of coastal water masses. Hydrobiologia 464, 99–105.

Yokouchi, Y., Hasebe, F., Fujiwara, M., Takashima, H., Shiotani, M., Nishi, N., Kanaya, Y., Hashimoto, S., Fraser, P., Toom-Sauntry, D., Mukai, H., Nojiri, Y. 2005. Correlation and emission ratios among bromoform, dibromochloromethane and dibromomethane in the atmosphere. J. Geophys. Res. Atmos. 110, D23309.

Yokouchi, Y., Saito, T., Zeng, J., Mukai, H., Montzka, S.A., 2017. Seasonal variation of bromocarbons at Hateruma Island, Japan: implications for global sources. J. Atmos. Chem. 74, 171–185.

Yvon-Lewis, S.A., Saltzman, E.S., Montzka, S.A., 2009. Recent trends in atmospheric methyl bromide: analysis of post-Montreal Protocol variability. Atmos. Chem. Phys. 9, 5963–5974.

Ziska, F., Quack, B., Abrahamsson, K., Archer, S.D., Atlas, E., Bell, T., Butler, J.H., Carpenter, L.J., Jones, C.E., Harris, N.R.P., Hepach, H., Heumann, K.G., Hughes, C., Kuss, J., Krüger,

K., Liss, P., Moore, R.M., Orlikowska, A., Raimund, S., Reeves, C.E., Reifenhäuser, W., Robinson, A.D., Schall, C., Tanhua, T., Tegtmeier, S., Turner, S., Wang, L., Wallace, D., Williams, J., Yamamoto, H., Yvon-Lewis, S.A., Yokouchi, Y., 2013. Global sea-to-air flux climatology for bromoform, dibromomethane and methyl iodide. Atmos. Chem. Phys. 13, 8915–8934.